The Rapid-Onset Chorioretinopathy Phenotype of ABCA4 Disease

Koji Tanaka, MD, PhD[1,2,*], **Winston Lee, MA**[1,*], **Jana Zernant, PhD**[1], **Kaspar Schuerch, MD**[1], **Lyam Ciccone, MD**[1], **Stephen H. Tsang, MD, PhD**[1,3], **Janet R. Sparrow, PhD**[1,3], and **Rando Allikmets, PhD**[1,3]

[1]Department of Ophthalmology, Columbia University, New York, New York

[2]Division of Ophthalmology, Department of Visual Sciences, Nihon University School of Medicine, Tokyo, Japan

[3]Department of Pathology and Cell Biology, Columbia University, New York, New York

Abstract

Purpose—To characterize patients affected by a uniquely severe, rapid-onset chorioretinopathy (ROC) phenotype of ABCA4 disease.

Design—Comparative cohort study.

Participants—Sixteen patients were selected from a large clinically diagnosed and genetically confirmed cohort (n = 300) of patients diagnosed with ABCA4 disease.

Main Outcome Measures—Phenotypic characteristics were assessed on color fundus photographs, short-wavelength autofluorescence (488-nm), and near-infrared autofluorescence (NIR-AF, 787-nm) images. Subfoveal thickness measurements were obtained from enhanced-depth imaging OCT. Generalized retinal function was determined with full-field electroretinogram (ffERG) testing, and lipofuscin accumulation was assessed by quantitative autofluorescence (qAF).

Results—All patients exhibited advanced disease features, including pigment migration in the macula and retinal vessel attenuation at an early age, and reported a symptomatic onset, on average, at 7.4 years (average for ABCA4 disease is 21.9 years, $P < 0.0001$). Deterioration of the macula was observed to begin with an intense, homogeneous signal on short-wavelength autofluorescence, which corresponds to an attenuated NIR-AF signal and progresses to a patchy, coalescing pattern of chorioretinal atrophy within the subsequent decade. Measurement of

choroidal thickness revealed a more rapid thinning of choriocapillaris with age of Sattler's layer compared with the rate in most other patients with ABCA4 disease ($P < 0.001$). Levels of qAF in the macula before atrophy were above both the 95% confidence intervals for healthy individuals and patients with Stargardt disease (STGD1) (>1000 qAF units). Severe attenuation of cone responses and notable decreases in rod responses were detected by ffERG. Sequencing of the *ABCA4* gene revealed exclusively deleterious, null mutations, including stop codons; frameshift deletions; variants in canonical splice sites, which completely abolish splicing; and known deleterious missense alleles.

Conclusions—The ROC phenotype is a unique classification of ABCA4 disease, which is caused by deleterious null biallelic ABCA4 mutations and is characterized by the rapid deterioration of retinal pigment epithelium and photoreceptor layers in the macula and significant choroidal thinning within the first 2 decades of life.

Stargardt disease (STGD1) is the most common juvenile-onset macular dystrophy affecting 1 in 5 of 10 000 people worldwide.[1] Since its discovery as the causative gene in 1997,[2] more than 800 disease-causing mutations within the coding (50 exons) and noncoding regions of the ATP Binding Cassette Subfamily A Member 4 (*ABCA4*, Mendelian Inheritance in Man #601691) gene have been reported,[3] giving rise to a large heterogeneous group of retinal dystrophies. As a result, the clinical variation of ABCA4 diseases is extensive and spans a wide spectrum of phenotypes, including occult maculopathy,[4] bull's eye maculopathy,[5,6] cone-rod dystrophy,[7,8] generalized choriocapillaris dystrophy,[9] and severe retinitis pigmentosa-like retinopathies.[7,10] The diagnostic criteria for ABCA4-associated disease encompasses several distinct features that are generally ubiquitous among affected patients. Dysfunction of the ABCA4 protein results in a high accumulation of bisretinoid lipofuscin[11] due to the inadequate handling of vitamin A aldehyde, with the result that the various phototoxic bisretinoids form in photoreceptor outer segments at an accelerated pace.[12,13]

The extent of genetic variability in *ABCA4* impedes the assessment of genotype–phenotype correlations; however, the abundance of data from patients harboring c.5882G>A (p.G1961E) has revealed its association with a confined maculopathy,[5] lower accumulation of lipofuscin (autofluorescence [AF]),[14,15] and the long-term preservation of cone and rod function. More severe phenotypes resulting in earlier symptomatic onset and faster disease progression have been described for other, more severe variants, such as the complex allele c.[1622T>C; 3113C>T] (p.[L541P; A1038V]) resulting in protein misfolding or the c.5461-10T>C intronic variant, which leads to exon skipping and, consequently, protein truncation.[16,17]

The characterization of heterogeneously presenting genetic disease subtypes contributes to diagnostic and prognostic accuracy and increases understanding of disease etiology. In the current article, a new phenotype of ABCA4 disease, termed "rapid-onset chorioretinopathy" (ROC) is described with respect to disease presentation, onset, progression, and genotype.

Methods

Patients and Clinical Evaluation

All study subjects provided consent before participating in the study under the protocol #AAAI9906 approved by the Institutional Review Board at Columbia University, and all study procedures adhered to tenets established by the Declaration of Helsinki. Study subjects were analyzed from a research database of 300 patients with the following enrollment criteria: (1) a clinical diagnosis of STGD1 by a retinal specialist at the Department of Ophthalmology, Columbia University, (2) harbor at least 2 expected disease-causing *ABCA4* mutations identified from next generation sequencing and (3) a comprehensive set of clinical data. Data included color fundus photographs, short wavelength (488 nm) and near infrared (787 nm) autofluorescence images, spectral-domain OCT scans and in most, full-field electroretinogram (ffERG) results. The ROC phenotype was clinically defined by an unusual but distinct characteristic on autofluorescence (488 nm) images for which the patients (n = 16) in the study cohort were selected. The selection criteria were (1) the presence, or remnant of, an intense, localized region of autofluorescence in the macula preceding a (2) rapid, heterogeneous pattern of RPE atrophy within the region of AF (Fig 1). Patients presenting at an advanced disease stage whereby atrophy extended beyond the posterior pole were not evaluated for inclusion as the above criteria could not be verified. After identifying individuals exhibiting this autofluorescence phenotype, further clinical parameters were compiled and subsequently analyzed against other patients in the ABCA4 disease database. All clinical data were obtained from complete ophthalmic and dilated fundus exams, which additionally included measurement of Snellen best corrected visual acuity (BCVA). Color fundus photographs were obtained with an FF 450plus Fundus Camera (Carl Zeiss Meditec AG, Jena, Germany). Spectral-domain (SD) OCT scans and corresponding infrared reflectance fundus images were acquired using a Spectralis HRA+OCT (or HRA+OCT) (Heidelberg Engineering, Heidelberg, Germany). Fundus AF images were obtained using a confocal scanning-laser ophthalmoscope (cSLO) (Heidelberg Retina Angiograph 2, Heidelberg Engineering, Dossenheim, Germany).

Full-field electroretinograms (ffERG) available for 13 of the 16 patients, were recorded using the Diagnosys Espion Electrophysiology System (Diagnosys LLC, Littleton, MA). Before acquisition, pupils were maximally dilated and measured before ffERG recording using tropicamide (1%) and phenylephrine hydrochloride (2.5%), and the corneas were anesthetized with proparacaine 0.5%. Silver-impregnated fiber electrodes (DTL; Diagnosys LLC, Littleton, MA) and Burian-Allen contact lens were used with a ground electrode on the forehead. Normative amplitude and implicit time ranges for each stimulus were provided by the Diagnosys system software. All procedures were performed using extended testing protocols outlined by the International Society for Clinical Electrophysiology of Vision standard.[18]

Analysis of Choroidal Layer Thickness

Choroidal thickness measurements were made on horizontal 9-mm enhanced-depth imaging OCT (EDI-OCT) scans through the fovea in all ROC study patients and compared to thicknesses of other ABCA4 disease patients from the preliminary cohort for whom foveal

EDI-OCT was available (n = 207). Patients with a refractive error >6 diopters were excluded to account for anatomic determinants of choroidal thickness. Thickness measurements were made at the subfoveal position in all subjects by 2 independent examiners (K.T. and L.C.) with the caliper tool on the Heidelberg Explorer (HEYEX) software. The delineation of the choriocapillaris, Sattler's layer (CS layer), and Haller's layer were assessed in accordance with the criteria defined by Wakatsuki et al.[19] The limited resolution of SD OCT hinders the visual separation of the choriocapillaris and Sattler's layers and as such, the region spanning the posterior edge of the RPE and small diameter vessels was defined as the choriocapillaris + Sattler's (C+S) layer. The region between posterior boundary of the C+S layer and the choroidal/scleral interface encompassing large diameter vessels was defined as Haller's layer. Total subfoveal choroidal thickness is defined as the sum of C+S and Haller's layers below the fovea.

The Mann–Whitney U and Fisher exact tests were performed to determine the significance of differences using the SPSS (version 21) software [IBM Corp, Armonk, NY]. Statistical significance is defined as P 0.05.

Quantitative Autofluorescence

Analysis of quantitative autofluorescence (qAF) was performed in both the right and left eyes of P3 and compared with the previously published cohort of ABCA4 disease patients and healthy eyes.[14,20] Protocols for the acquisition of qAF images in P3 met all quality standards necessary for quantification as previously described.[14,21]

Sequencing and Variant Analyses

All 50 exons and exon–intron boundaries of the *ABCA4* gene (MIM 601691, NM_000350.2) were amplified using Illumina TruSeq Custom Amplicon protocol (Illumina, San Diego, CA), followed by sequencing on the Illumina MiSeq platform. The next-generation sequencing reads were analyzed and compared with the *ABCA4* reference sequence NG 009073.1, using the variant discovery software NextGENe (SoftGenetics LLC, State College, PA). All detected possibly disease-associated variants were confirmed by Sanger sequencing. Nucleotide positions and protein translation correspond to CCDS747.1 and NP 000341.2, respectively. Nucleotide numbering uses the A of the ATG translation initiation start site as nucleotide 1. The allele frequencies of all variants were compared with the Exome Aggregation Consortium database (Cambridge, MA; http://exac.broadinstitute.org; accessed December 2016). All *ABCA4* variants reported in this article were submitted to the *ABCA4* LSDB (http://www.lovd.nl/ABCA4) at the Leiden Open Variation Database 3.0 (available at: http://www.lovd.nl/3.0/home).

The predicted effect of each detected coding variant in *ABCA4* was assessed using Aligned GVHD (available at: http://agvgd.hci.utah.edu/agvgd_input.php),[22] Sorting Intolerant from Tolerant (SIFT) (available at: www.sift.jcvi.org/),[23] PolyPhen2 (available at: http://genetics.bwh.harvard.edu/pph2/index.shtml),[24] Mutation Taster (available at: http://www.mutationtaster.org/),[25] and Mendelian Clinically Applicable Pathogenicity Score (available at: http://bejerano.stanford.edu/mcap/).[26] Predicted effects on splicing of all the

missense and intronic variants were assessed with the Human Splicing finder program version 2.4.1 (available at: www.umd.be/HSF/).

Results

Clinical phenotypes within the overall cohort (n = 300) predominantly exhibited characteristics consistent with *ABCA4* disease including centrifugal development of flecks beginning in the macula, well-delineated lesions of dark atrophy enlarging over time and posterior pole atrophy in a proportion of older, more advanced cases. The assessment of autofluorescence images identified an unusual phenotype (ROC, n = 16) characterized by a dense, homogenous distribution of autofluorescence concentrated across the macula which subsequently progresses to a muddled pattern of atrophy (Fig 1). Remnants of the macular AF are apparent after subsequent atrophy. The pattern of homogenous AF in the macula preceding atrophy spatially corresponds to reduced signal on NIR-AF indicating a widespread loss of underlying RPE in this region while nascent flecks develop in the periphery over time (Fig 2).

Demographic and clinical characteristics of the ROC cohort are summarized in Table 1. Age at examination ranged from 7 to 41 years of age (mean age, 23.4 years). In all cases, disease (symptomatic) onset was reported in the first decade of life (mean, 7.0 years). Measured best-corrected visual acuity ranged from 20/200 to counting fingers (average logarithm of the minimum angle of resolution, right eye = 1.48; left eye = 1.41). Funduscopic examinations were remarkable for features associated with advanced retinal disease including varying degrees of intra-retinal pigment in the macula in 12 of 16 cases (75%) beginning at 16 years of age (P5). Extensive bone spicule pigment patterns were apparent in 3 patients (P7, P8, and P9) (Fig 3). Visible attenuation of the retinal vasculature was evident in all except 3 cases (81%) (Fig 3, insets), and loss of complete peripapillary sparing is seen in 7 patients (44%). A statistical comparison of clinical characteristics described above between ROC other ABCA4 disease patients within the initial cohort are summarized in Table 2. Full-field ERG testing of ROC patients revealed moderate to severe generalized cone dysfunction in all 13 patients for whom these data were available while 12 of the 13 (92%) cases were also found to have varying degrees of functional loss in the rod responses (Fig 4).

Differences in the total and individual choroidal layers between ROC patients and other ABCA4 patients were also assessed. Total subfoveal choroidal thickness and Haller's layer thickness revealed no significant difference between ROC and other ABCA4 cases (Fig 5). However, CS layer thickness exhibited a trend toward thinning ($P = 0.07$), and CS layer/Haller's layer ratio was significantly lower than in other ABCA4 cases ($P = 0.001$). Intraclass correlation coefficients indicated good agreement between measurers of CS (0.748) and Haller (0.863) layer thicknesses.

Measurement of qAF was only possible in P3 due to of the excessive degeneration in the macula in other study patients. Mean levels of qAF results in both eyes of P3 were compared with the ABCA4 cohort previously reported by Burke et al[14] and the healthy eyes of white subjects.[20] Although qAF values in the majority of the ABCA4 subjects were above the 95%

confidence intervals for healthy eyes, they were, in comparison, substantially higher in P3 (right eye, 1129 qAF units; left eye, 1132 qAF units) (Fig 6).

The genotypic profile of ROC patients consisted of 21 unique variants predicted or previously described to be null *ABCA4* alleles. A total of 21 unique variants were detected. Mutations included 6 noncoding variants predicted to completely abolish splicing, including c.5461-10T>C, which has been reported to result in the skipping of exon 39 and 40 in mRNA (Table 3). Four small deletions of 1–4 nucleotides resulting frameshifts and 7 nonsense variants resulting in premature stop codons were also detected. All missense variants, c.1609C>T (p.R537C), c.1804C>T (p.R602W), c.2300T>A (p.V767D), c. 4139C>T (p.P1380L), and c.6317G>A (p.R2106H), were predicted strongly deleterious by Mendelian Clinically Applicable Pathogenicity (score 0.290–0.501) and nearly unanimously damaging or deleterious by Polyphen-2, AGVGD class, SIFT, and MutationTaster. Of note, 6 disease alleles resulted in arginine substitutions (all predicted deleterious or disease-causing by both SIFT and MutationTaster) or stop-gain, in comparison, variants.

Discussion

The etiological events of ABCA4 dysfunction give rise to a diverse group of retinal phenotypes classified largely according to prognostic trajectory and to a lesser extent genotypic differences. Differentiating disease phenotypes improves clinical management and provides a top-down approach to understanding disease pathogenesis.

After reviewing data from 300 patients with confirmed biallelic ABCA4 disease, the most recognizable criteria that differentiated the ROC phenotype was the distinct clinical presentation in the macula, particularly in autofluorescence imaging. Increased AF (lipofuscin) levels are central to the pathology of ABCA4 disease and can manifest as a dark choroid[15] in fundus angiography or increased qAF levels as previously reported.[6,14] Correlations with genotype have been observed as patients with deleterious mutations, such as the complex allele p.[L541P/A1038V], exhibit higher qAF levels and at a younger age relative to more moderate to no significant elevation in patients with the milder p.G1961E allele.[14] The genotypic profile of this cohort consists almost entirely of deleterious mutations, including 7 nonsense variants (1 as a complex allele), 6 deletions, 8 variants in canonical splice sites, and a few missense variants that are predicted deleterious (p.R537C, p.R602W, p.P1380L, and p.R2106H). The qAF levels in P3, an individual harboring 2 deleterious *ABCA4* alleles, were not only above age-matched healthy eyes, but at >1000 qAF-units, higher than all other patients in the entire recessive STGD1 cohort.[6,14]

This region of intense AF in the macula simultaneously exhibits a spatially corresponding loss of the ellipsoid layer on spectral-domain OCT and attenuation of the NIR-AF signal indicating a preceding loss of underlying RPE[27,28] that is analogous to the sequence of events in the formation of autofluorescent flecks.[29] The intense AF signal from this region thus may originate at least predominantly from lipofuscin-laden photoreceptors amid ongoing degeneration. Significant RPE involvement at an early stage in ROC is further corroborated by the choroidal thinning observed in this cohort. The role of RPE in maintaining choroidal integrity, particularly the choriocapillaris through vascular endothelial

growth factor, is known,[30] and several studies have reported choroidal thinning in ABCA4 disease.[31,32] More specifically, this study showed selective thinning of Sattler's layer in the ROC group compared with other patients with ABCA4 disease, which may be an extension of the process affecting the choriocapillaris. More rigorous studies will be necessary to understand the choriopathology of ABCA4 disease; however, the current findings support the severity of outer retinal loss in ROC.

Other clinical attributes in ROC include those associated with advanced retinal disease stages seen in both ABCA4 and other retinal degenerative diseases, such as the thinning and attenuation of retinal vessels, visible pigment migration and aggressive atrophy of the outer retina. Unlike the well-defined atrophy lesions in ABCA4 disease that have been reported to enlarge in size at a rate of 0.5 to 2.0 mm^2/ year,[33,34] atrophy in ROC appears to begin early and progress rapidly in a disorganized, multifocal pattern similar to patients with rapid functional decline.[35] The resultant presentation is a diffuse pattern of multifocal atrophy circumscribed by a border or ring of residual increased AF as seen in the majority of cases presented in this cohort. The group 3 ffERG classification by Lois et al,[36] defined as significant cone dysfunction along with rod abnormalities, is another clinical attribute of ROC as all but 1 patient in this cohort are in the group 3 ffERG classification. Furthermore, progression to group 3 functional loss is detected at the clinical presentation age of 23.2 years (standard deviation, 9.93) compared with 40.3 years (standard deviation, 1.30) reported by Fujinami et al.[35]

The presumed complete absence of functional ABCA4 protein in the retina produces an expected severe phenotype in patients encompassing conditions such as cone-rod dystrophy[7,8,37–41] and retinitis pigmentosa,[10,41–43] among others. The rapid attenuation of generalized cone function relative to rod loss and trajectory of visual decline indicate that ROC is a subvariant of cone-rod dystrophy; however, not all cone-rod dystrophy cases in our database exhibit the precise ROC phenotype. Patients in our ABCA4 database harboring 2 null or deleterious alleles (~16%) occupy a range of severe phenotypes of which ROC represents only a third (~32%). The remainder consists of other more typical cone-rod and retinitis pigmentosa-like cases. Ascertaining underlying further genotype differences among these 3 groups was not possible given the relatively small numbers of cases in each phenotype group, but the difference may involve other systemic or environmental factors or genetic modifiers. Phenotypic variability amongst individuals of similar genetic backgrounds or identical genotypes (siblings) may substantiate further investigation but is beyond the scope of this study.[44,45]

In summary, the ROC phenotype in ABCA4 disease is a distinct sub-phenotype in patients who lack any functional ABCA4 protein, characterized by an early onset (<10 years of age) and a rapid progression to advanced disease. The span of progression occurs within 2 to 3 decades beginning with rapid accumulation of bisretinoid lipofuscin in photoreceptor cells, secondary deposition in the RPE, and followed by widespread RPE death in the macula. Subsequent thinning of the choriocapillaris and CS layer, diffuse, multifocal atrophy, and generalized electrophysiologic dysfunction lead to significant visual decline at a much younger age than in other cases of ABCA4 disease.

Acknowledgments

Abbreviations and Acronyms

AF	autofluorescence
CS	choriocapillaris and Sattler's layer
ffERG	full-field electroretinogram
NIR-AF	near-infrared auto-fluorescence
qAF	quantitative autofluorescence
ROC	rapid-onset chorioretinopathy
RPE	retinal pigment epithelium
SIFT	Sorting Intolerant from Tolerant
STGD1	Stargardt disease

References

1. Blacharski, PA. Fundus flavimaculatus. In: Newsome, DA., editor. Retinal Dystrophies and Degenerations. New York: Raven Press; 1988. p. 135-159.

2. Allikmets R, Singh N, Sun H, et al. A photoreceptor cell-specific ATP-binding transporter gene (ABCR) is mutated in recessive Stargardt macular dystrophy. Nat Genet. 1997; 15:236–246. [PubMed: 9054934]

3. Cornelis SS, Bax NM, Zernant J, et al. In silico functional meta-analysis of 5,962 ABCA4 variants in 3,928 retinal dystrophy cases. Hum Mutat. 2017; 38:400–408. [PubMed: 28044389]

4. Noupuu K, Lee W, Zernant J, et al. Structural and genetic assessment of the ABCA4-associated optical gap phenotype. Invest Ophthalmol Vis Sci. 2014; 55:7217–7226. [PubMed: 25301883]

5. Cella W, Greenstein VC, Zernant-Rajang J, et al. G1961E mutant allele in the Stargardt disease gene ABCA4 causes bull's eye maculopathy. Exp Eye Res. 2009; 89:16–24. [PubMed: 19217903]

6. Duncker T, Tsang SH, Lee W, et al. Quantitative fundus autofluorescence distinguishes ABCA4-associated and non-ABCA4-associated bull's-eye maculopathy. Ophthalmology. 2015; 122:345–355. [PubMed: 25283059]

7. Cremers FP, van de Pol DJ, van Driel M, et al. Autosomal recessive retinitis pigmentosa and cone-rod dystrophy caused by splice site mutations in the Stargardt's disease gene ABCR. Hum Mol Genet. 1998; 7:355–362. [PubMed: 9466990]

8. Maugeri A, Klevering BJ, Rohrschneider K, et al. Mutations in the ABCA4 (ABCR) gene are the major cause of autosomal recessive cone-rod dystrophy. Am J Hum Genet. 2000; 67:960–966. [PubMed: 10958761]

9. Bertelsen M, Zernant J, Larsen M, et al. Generalized chorio-capillaris dystrophy, a distinct phenotype in the spectrum of ABCA4-associated retinopathies. Invest Ophthalmol Vis Sci. 2014; 55:2766–2776. [PubMed: 24713488]

10. Martinez-Mir A, Paloma E, Allikmets R, et al. Retinitis pig-mentosa caused by a homozygous mutation in the Stargardt disease gene ABCR. Nat Genet. 1998; 18:11–12. [PubMed: 9425888]

11. Cideciyan AV, Aleman TS, Swider M, et al. Mutations in ABCA4 result in accumulation of lipofuscin before slowing of the retinoid cycle: a reappraisal of the human disease sequence. Hum Mol Genet. 2004; 13:525–534. [PubMed: 14709597]

12. Sparrow JR, Gregory-Roberts E, Yamamoto K, et al. The bisretinoids of retinal pigment epithelium. Prog Retin Eye Res. 2012; 31:121–135. [PubMed: 22209824]

13. Sparrow JR, Parish CA, Hashimoto M, Nakanishi K. A2E, a lipofuscin fluorophore, in human retinal pigmented epithelial cells in culture. Invest Ophthalmol Vis Sci. 1999; 40:2988–2995. [PubMed: 10549662]

14. Burke TR, Duncker T, Woods RL, et al. Quantitative fundus autofluorescence in recessive Stargardt disease. Invest Oph-thalmol Vis Sci. 2014; 55:2841–2852.

15. Fishman GA, Stone EM, Grover S, et al. Variation of clinical expression in patients with Stargardt dystrophy and sequence variations in the ABCR gene. Arch Ophthalmol. 1999; 117:504–510. [PubMed: 10206579]

16. Sangermano R, Bax NM, Bauwens M, et al. Photoreceptor progenitor mRNA analysis reveals exon skipping resulting from the ABCA4 c.5461-10T–>C mutation in Stargardt disease. Ophthalmology. 2016; 123:1375–1385. [PubMed: 26976702]

17. Zhang N, Tsybovsky Y, Kolesnikov AV, et al. Protein misfolding and the pathogenesis of ABCA4-associated retinal degenerations. Hum Mol Genet. 2015; 24:3220–3237. [PubMed: 25712131]

18. McCulloch DL, Marmor MF, Brigell MG, et al. ISCEV Standard for full-field clinical electroretinography (2015 update). Doc Ophthalmol. 2015; 130:1–12.

19. Wakatsuki Y, Shinojima A, Kawamura A, Yuzawa M. Correlation of aging and segmental choroidal thickness measurement using swept source optical coherence tomography in healthy eyes. PLoS One. 2015; 10:e0144156. [PubMed: 26632821]

20. Greenberg JP, Duncker T, Woods RL, et al. Quantitative fundus autofluorescence in healthy eyes. Invest Ophthalmol Vis Sci. 2013; 54:5684–5693. [PubMed: 23860757]

21. Delori F, Greenberg JP, Woods RL, et al. Quantitative measurements of autofluorescence with the scanning laser ophthalmoscope. Invest Ophthalmol Vis Sci. 2011; 52:9379–9390. [PubMed: 22016060]

22. Tavtigian SV, Deffenbaugh AM, Yin L, et al. Comprehensive statistical study of 452 BRCA1 missense substitutions with classification of eight recurrent substitutions as neutral. J Med Genet. 2006; 43:295–305. [PubMed: 16014699]

23. Ng PC, Henikoff S. Predicting deleterious amino acid substitutions. Genome Res. 2001; 11:863–874. [PubMed: 11337480]

24. Adzhubei IA, Schmidt S, Peshkin L, et al. A method and server for predicting damaging missense mutations. Nat Methods. 2010; 7:248–249. [PubMed: 20354512]

25. Schwarz JM, Rodelsperger C, Schuelke M, Seelow D. MutationTaster evaluates disease-causing potential of sequence alterations. Nat Methods. 2010; 7:575–576. [PubMed: 20676075]

26. Jagadeesh KA, Wenger AM, Berger MJ, et al. M-CAP eliminates a majority of variants of uncertain significance in clinical exomes at high sensitivity. Nat Genet. 2016; 48:1581–1586. [PubMed: 27776117]

27. Keilhauer CN, Delori FC. Near-infrared autofluorescence imaging of the fundus: visualization of ocular melanin. Invest Ophthalmol Vis Sci. 2006; 47:3556–3564. [PubMed: 16877429]

28. Duncker T, Marsiglia M, Lee W, et al. Correlations among near-infrared and short-wavelength autofluorescence and spectral-domain optical coherence tomography in recessive Stargardt disease. Invest Ophthalmol Vis Sci. 2014; 55:8134–8143. [PubMed: 25342616]

29. Sparrow JR, Marsiglia M, Allikmets R, et al. Flecks in recessive Stargardt disease: short-wavelength autofluorescence, near-infrared autofluorescence, and optical coherence tomography. Invest Ophthalmol Vis Sci. 2015; 56:5029–5039. [PubMed: 26230768]

30. Saint-Geniez M, Kurihara T, Sekiyama E, et al. An essential role for RPE-derived soluble VEGF in the maintenance of the choriocapillaris. Proc Natl Acad Sci U S A. 2009; 106:18751–18756. [PubMed: 19841260]

31. Muller PL, Fimmers R, Gliem M, et al. Choroidal alterations in ABCA4-related retinopathy. Retina. 2017; 37:359–367. [PubMed: 27414126]

32. Nunes RP, Rosa PR, Giani A, et al. Choroidal thickness in eyes with central geographic atrophy secondary to Stargardt disease and age-related macular degeneration. Ophthalmic Surg Lasers Imaging Retina. 2015; 46:814–822. [PubMed: 26431296]

33. Chen B, Tosha C, Gorin MB, Nusinowitz S. Analysis of autofluorescent retinal images and measurement of atrophic lesion growth in Stargardt disease. Exp Eye Res. 2010; 91:143–152. [PubMed: 20398653]

34. Fujinami K, Lois N, Mukherjee R, et al. A longitudinal study of Stargardt disease: quantitative assessment of fundus autofluorescence, progression, and genotype correlations. Invest Ophthalmol Vis Sci. 2013; 54:8181–8190. [PubMed: 24265018]

35. Fujinami K, Lois N, Davidson AE, et al. A longitudinal study of Stargardt disease: clinical and electrophysiologic assessment, progression, and genotype correlations. Am J Ophthalmol. 2013; 155:1075–1088. e13. [PubMed: 23499370]

36. Lois N, Holder GE, Bunce C, et al. Phenotypic subtypes of Stargardt macular dystrophy-fundus flavimaculatus. Arch Ophthalmol. 2001; 119:359–369. [PubMed: 11231769]

37. Birch DG, Peters AY, Locke KL, et al. Visual function in patients with cone-rod dystrophy (CRD) associated with mutations in the ABCA4(ABCR) gene. Exp Eye Res. 2001; 73:877–886. [PubMed: 11846518]

38. Ducroq D, Rozet JM, Gerber S, et al. The ABCA4 gene in autosomal recessive cone-rod dystrophies. Am J Hum Genet. 2002; 71:1480–1482. [PubMed: 12515255]

39. Kitiratschky VB, Grau T, Bernd A, et al. ABCA4 gene analysis in patients with autosomal recessive cone and cone rod dystrophies. Eur J Hum Genet. 2008; 16:812–819. [PubMed: 18285826]

40. Littink KW, Koenekoop RK, van den Born LI, et al. Homozygosity mapping in patients with cone-rod dystrophy: novel mutations and clinical characterizations. Invest Ophthalmol Vis Sci. 2010; 51:5943–5951. [PubMed: 20554613]

41. Klevering BJ, Maugeri A, Wagner A, et al. Three families displaying the combination of Stargardt's disease with cone-rod dystrophy or retinitis pigmentosa. Ophthalmology. 2004; 111:546–553. [PubMed: 15019334]

42. Mullins RF, Kuehn MH, Radu RA, et al. Autosomal recessive retinitis pigmentosa due to ABCA4 mutations: clinical, pathologic, and molecular characterization. Invest Ophthalmol Vis Sci. 2012; 53:1883–1894. [PubMed: 22395892]

43. Zhang Q, Zulfiqar F, Xiao X, et al. Severe autosomal recessive retinitis pigmentosa maps to chromosome 1p13.3-p21.2 between D1S2896 and D1S457 but outside ABCA4. Hum Genet. 2005; 118:356–365. [PubMed: 16189710]

44. Lois N, Holder GE, Fitzke FW, et al. Intrafamilial variation of phenotype in Stargardt macular dystrophy-fundus flavimaculatus. Invest Ophthalmol Vis Sci. 1999; 40:2668–2675. [PubMed: 10509664]

45. Burke TR, Tsang SH, Zernant J, et al. Familial discordance in Stargardt disease. Mol Vis. 2012; 18:227–233. [PubMed: 22312191]

Rapid-Onset Chorioretinopathy (*ABCA4*)
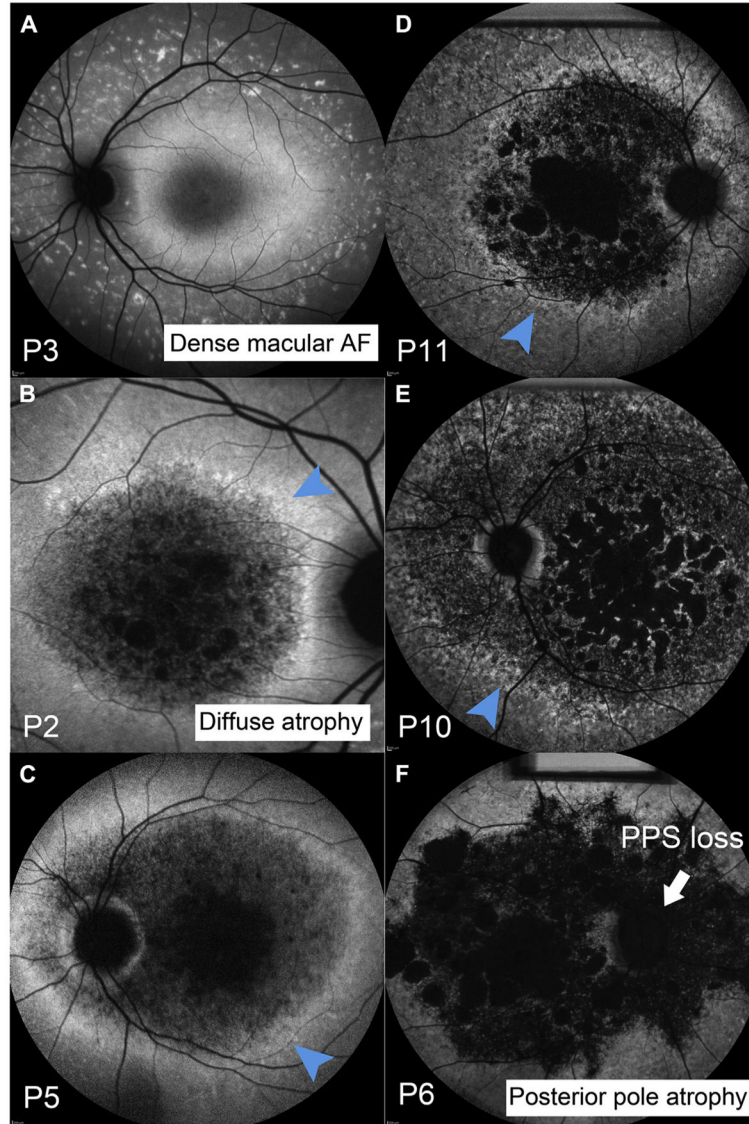
Figure 1.
Autofluorescence (AF) imaging in patients exhibiting the rapid-onset chorioretinopathy (ROC) phenotype of *ABCA4* disease. **A**, Homogenously elevated distribution of AF is apparent at an early disease stage in P3 (age 10 years) with nascent fleck development in the mid-periphery. **B** and **C**, The central region of elevated AF proceeds to diffuse patches of atrophy leaving behind a residual "ring of AF" (*blue arrowhead*) near the vascular arcades in P2, P5, P10, and P11. **D**–**F**, The loss of peripapillary sparing (PPS, *white arrow*) (P6) and multiple atrophic lesions coalesce and expand beyond the macula (P6, P10 and P11).
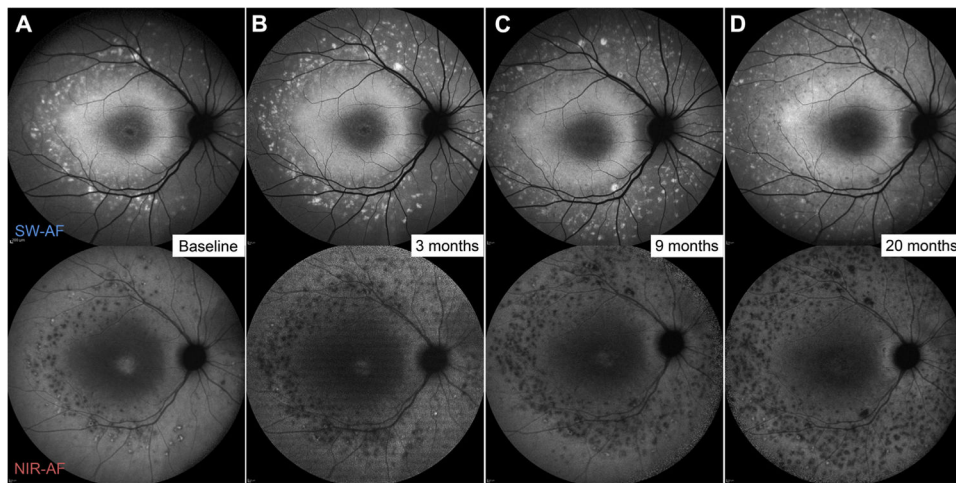
Figure 2.
Serial short-wavelength autofluorescence (SW-AF) (488-nm) and near-infrared autofluorescence (NIR-AF, 787-nm) in a 10-year-old (P3) exhibiting the early stage of the rapid-onset chorioretinopathy (ROC) phenotype of *ABCA4* disease. The dense, homogenous region of SW-AF in the macula corresponds to an attenuated signal of NIR-AF indicating underlying retinal pigment epithelium (RPE) loss. Fleck development and progression are apparent in the mid-periphery overtime.

Figure 3.
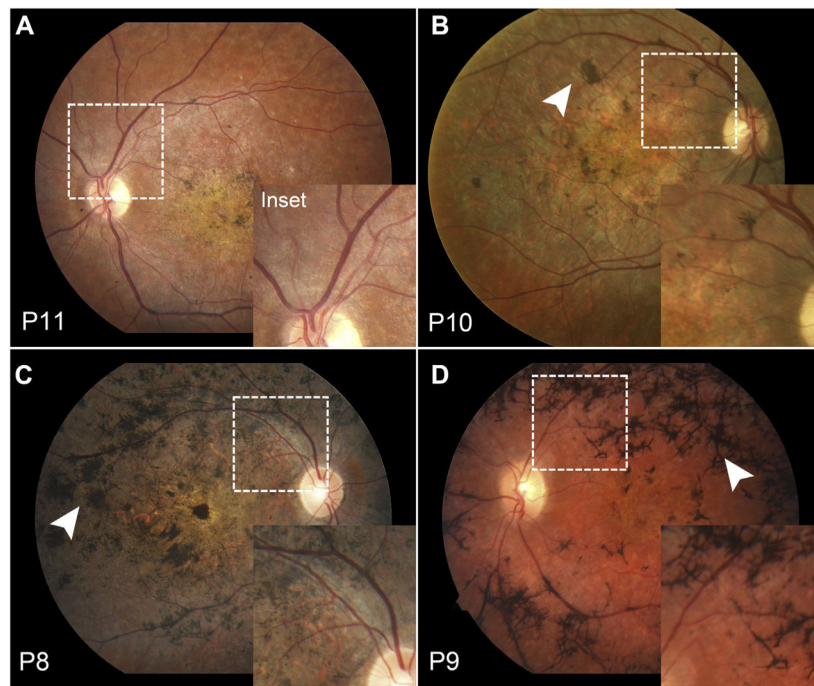Early attenuation of the retinal vasculature and variable pigment migration in the rapid-onset chorioretinopathy (ROC) phenotype of *ABCA4* disease. (**A**) Thinning of the retinal vasculature (*dotted boxes*) is apparent as early as the third decade and can be accompanied by a range of pigment migration (*white arrowheads*) from early nummular (**B**, **C**) to advanced (**D**) bone-spicule deposition.
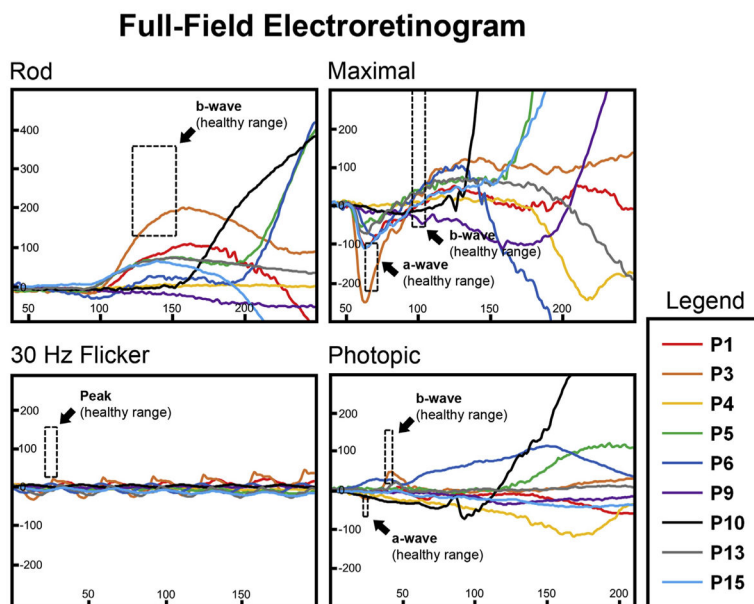
Figure 4.
Full-field electroretinogram results in patients exhibiting the rapid-onset chorioretinopathy (ROC) phenotype of ABCA4 disease. Rod, maximal, 30 Hz flicker and photopic scans of the right eye of representative patients are overlaid. Normal peak amplitude and implicit time ranges are delineated by the dashed line boxes.
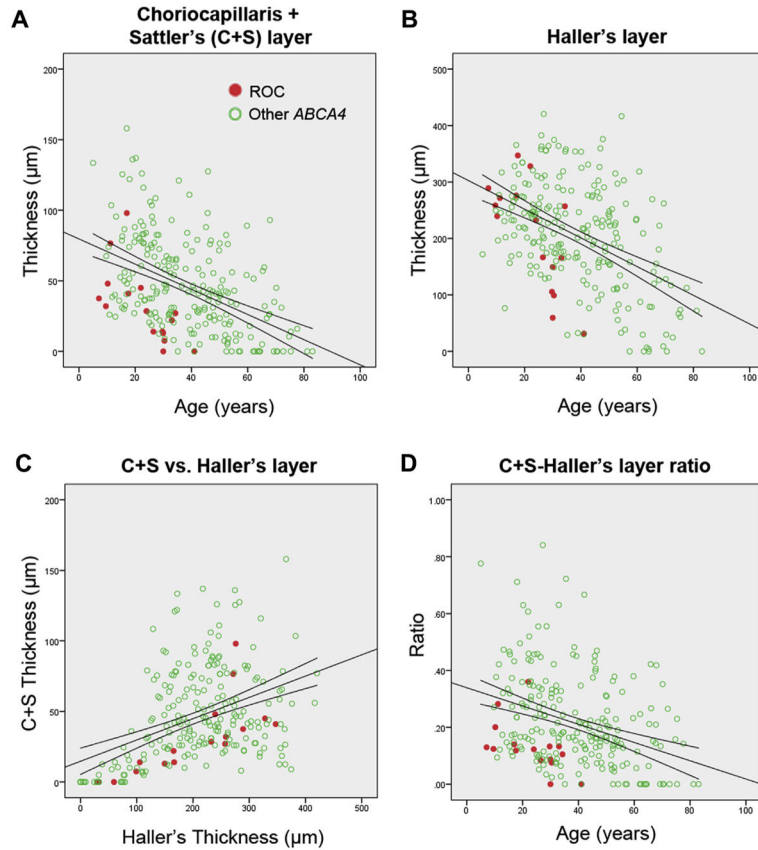
Figure 5.
Subfoveal thickness analysis of choroidal sublayers in patients with rapid-onset chorioretinopathy (ROC) phenotype (*red circles*) and other ABCA4 disease (*unfilled green circles*). **A**, Layers due to the choriocapillaris and Sattler's layer (CS) were found to fall below the 95% confidence interval with time compared with corresponding patients with ABCA4 disease. **B**, Thinning of Haller's layer was significant at a more advanced age but (**C, D**) in a more severe manner when compared with the CS layer.

Figure 6.
Quantitative autofluorescence (qAF) in rapid-onset chorioretinopathy (ROC) phenotype compared with Stargardt disease (STGD1) and healthy retinae. Increasing qAF levels are observed in healthy eyes (*gray circles*) with age. Stargardt disease levels fall above the 95% confidence interval (CI) of healthy eyes (*dotted lines*) but below the retina of P3 who exhibited >1000 qAF units in both eyes.

Table 1

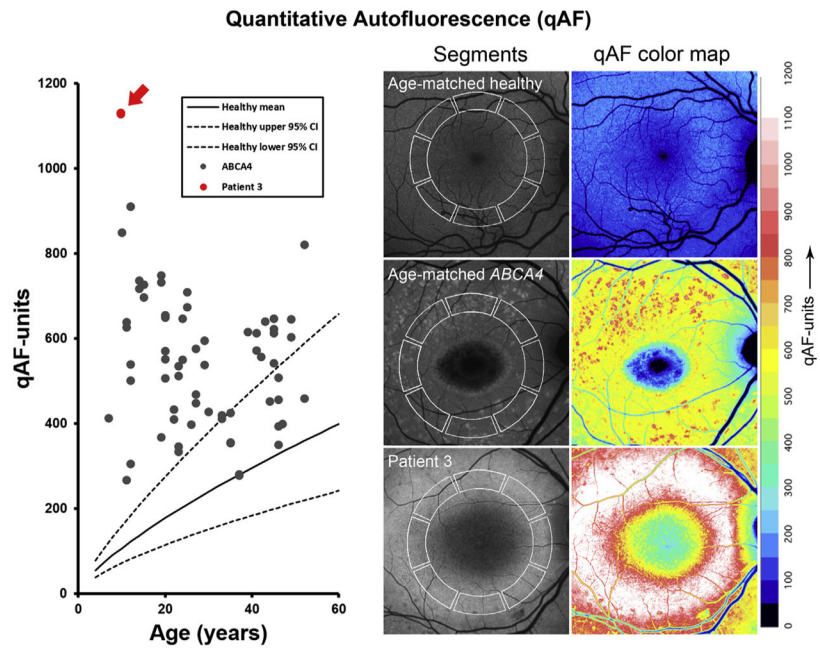Demographic, Clinical, and Genetic Characteristics of Patients with the Rapid-Onset Chorioretinopathy Phenotype of ABCA4 Disease

Patient	Age (yrs)	Gender	Onset Age (yrs)	Race/ Ethnicity	Pigment Migration	Outer Retinal Atrophy	Snellen BCVA OD	Snellen BCVA OS	logMAR BCVA OD	logMAR BCVA OS	ffERG Scotopic	ffERG Photopic	ABCA4 Variation Mutation 1	ABCA4 Variation Mutation 2
1†	7	F	3	Asian	−	−	20/800	20/800	1.60	1.60	→	↓↓	p.R408*	p.F1417del
2	10	M	7	White	−	+	20/400	20/400	1.30	1.30	→	→	p.L296fs	p.R537C
3	10	F	10	White	−	−	20/300	20/200	1.18	1.00	WNL	→	c.5312+1G>A	p.R2030*
4†	14	M	4	Asian	−	−	20/800	20/800	1.60	1.60	↓↓	↓↓↓	p.R408*	p.F1417del
5	16	M	6	Asian	+	+	20/400	20/400	1.30	1.30	→	↓↓	p.R408*	p.T1979fs
6	17	M	5	White	+	+	CF	20/400	2.00	1.30	NR	↓↓	p.[Y245*/V767D]	
7	22	M	7	Hispanic	+	+	20/400	20/400	1.30	1.30	NR	NR	p.R602W	p.C641*
8*	26	M	9	White	+	+	20/400	20/400	1.30	1.30	NR	NR	c.571-1G>T	c.2160+1G>C
9*	27	F	9	White	+	+	20/400	20/400	1.30	1.30	↓↓	↓↓↓	c.571-1G>T	c.2160+1G>C
10	29	M	8	White	+	+	CF	CF	2.00	2.00	↓↓	↓↓↓	p.R602W	p.R1300*
11	29	F	7	White	+	+	CF	20/400	2.00	1.30	→	NR	p.T1346fs	p.T1346fs
12	30	F	6	White	+	+	20/200	20/250	1.00	1.10	NR	NR	c.5461-10T>C	c.1239+1G>C
13	30	F	9	Hispanic	+	+	20/400	20/400	1.30	1.30	→	↓↓	p.S1185*	p.R2106H
14	33	M	10	White	+	+	20/400	20/800	1.30	1.60	NR	NR	p.W31*	p.P1380L
15	34	M	10	White	+	+	20/300	20/400	1.18	1.30	→	↓↓↓	p.P1380L	p.P1380L
16	41	F	9	White	+	+	CF	CF	2.00	2.00	↓↓	↓↓↓	c.5018+2T>C	c.5018+2T>C

BCVA = best-corrected visual acuity; CF = counting fingers; F = female; logMAR = logarithm of the minimum angle or resolution; M = male; OD = right eye, OS = left eye.

*
Sibling pair P8 and P9.

†
Sibling pair P1 and P4.

Table 2

Statistical Comparison of Clinical Characteristics between the Rapid-Onset Chorioretinopathy Phenotype and ABCA4 Disease

	ROC	Overall ABCA4 Disease Cohort	P Value	Age-Matched ABCA4 Disease Cohort	P Value
Cases (n)	16	284	—	127	d
Mean age (yrs)	23.4	39.6	6×10^{-6}	23.4	0.977
Onset age (yrs)	7.3	21.9	8×10^{-28}	15.1	3×10^{-13}
Pigment migration (%)	75%	50%	0.308	27%	**0.018**
Outer retinal atrophy (%)	81%	58%	0.431	36%	**0.046**

ROC = rapid-onset chorioretinopathy.

Bold text indicates statistical significance (*P* 0.05).

Table 3

Analysis of *ABCA4* (NM_000350.2) Variants in the Rapid-Onset Chorioretinopathy Phenotype of ABCA4 Disease by Predictive Programs

Exon/Intron	Nucleotide Change	Protein Variant	Allele Count	Allele Frequency (%) in Total Population	Polyphen-2 Prediction	AGVGD Class	SIFT Prediction	Taster Prediction	M-CAP Prediction	Predicted Effect on Splicing
2	c.93G>A	p.W31[†]	1	4.07E-06						
IVS5	c.571-1G>T	p.?	1							Change at acceptor site 1 bps downstream: −100%
6	c.733T>C[*]	p.Y245[†]	1	8.24E-06					0.284	
8	c.885delC	p.L296fs	1	4.13E-03						
9	c.1222C>T	p.R408[†]	2	2.47E-03						
IVS9	c.1239+1G>C	p.?	1	8.20E-04						Change at donor site 1 bps upstream: −100%
12	c.1609C>T	p.R537C	1	1.65E-03	Probably damaging	C45	Deleterious	Disease causing	0.418	
13	c.1804C>T	p.R602W	2	5.04E-03	Possibly damaging	C65	Deleterious	Disease causing	0.498	
13	c.1923C>A	p.C641[†]	1	4.07E-06						
IVS14	c.2160+1G>C	p.?	1							Change at donor site 1 bps upstream: −100%
24	c.3554_3555CC>GA	p.S1185[†]	1							
27	c.3898C>T	p.R1300[†]	1	3.37E-03						
27	c.4036_4037delAC	p.T1346fs	2							
28	c.4139C>T	p.P1380L	3	2.01E-02	Probably damaging	C65	Deleterious	Disease causing	0.391	
28	c.4249_4251delTTC	p.F1417del	1							
IVS35	c.5018+2T>C	p.?	2							Change at donor site 2 bps upstream: −100%
IVS37	c.5312+1G>A	p.?	1	3.20E-05						Change at donor site 1 bps upstream: −100%
IVS38	c.5461-10T>C	p.?	1	2.28E-04						Sangermano et al[16]
43	c.5935delA	p.T1979fs	1							
44	c.6088C>T	p.R2030[†]	1	2.84E-05						
46	c.6317G>A	p.R2106H	1	7.22E-06	Probably damaging	C25	Deleterious	Disease causing	0.29	

AGVGD = Align-Grantham Variation and Grantham Deviation; bps = base pairs; ExAC = Exome Aggregation Consortium; IVS = intervening sequence; M-CAP = Mendelian Clinical Applicable Pathogenicity; SIFT = Sorting Intolerant from Tolerant.

*
Constituent of complex allele (Table 1).

†
Allele count excluding familial pair.